J. Inst. Eng. India Ser. C (February 2022) 103(1):135–142
https://doi.org/10.1007/s40032-021-00660-4

REVIEW PAPER

Designing Nanostructured Materials through Self-Assembly and their Applications

Hitasha Shahi[1] · Jasveer Kaur[1] · Sonalika Vaidya[1]

Received: 18 March 2020 / Accepted: 8 January 2021 / Published online: 29 January 2021

Abstract Self-assembly is a process where particles aggregate together into well-defined structures, leading to the formation of hierarchical structures and nanostructures with varied morphologies. Various non-covalent interactions, which include H-bonding, electrostatic, van der Waals and hydrophobic interactions, are responsible for the formation of assembled structures. Other factors such as the nature of the solvent, temperature and pressure also affect the nature of the assembly. These assemblies lead to coupling effect, which results in changes in the physical properties. The assembled structures have found potential applications in the area of catalysis including photocatalysis and electrocatalysis, Li-ion batteries, sensing, biological applications. This review article focuses on giving a brief glimpse of the self-assembled structures, various forces of interactions leading to self-assembly, their effect on physical properties and applications.

Keywords Self-assembly · Nanostructures · Interactions · Physical properties · Applications

Introduction

Self-assembly is a process by which molecules or the components are arranged by itself into an organized structure or a pattern through non-covalent interactions. Self-assembly of micro- and nanostructured building blocks leads to the formation of hierarchical structures and results in high surface area, porosity and open active sites, which makes them very attractive in the area of catalysis. It provides an important role in providing a new route for the formation of materials with exciting properties. Self-assembly involves diffusion followed by nucleation, growth and at the end, Ostwald ripening. It is both kinetically and thermodynamically driven. Kinetically driven self-assembly involves diffusion, whereas thermodynamically driven is related to free energy (either entropic or enthalpic or both). The rate of growth of the nanostructures depends on both kinds of processes.

There have been reviews on self-assembly by Genix et al. [1], Arun et al. [2], Hwa et al. [3], Zhihong et al. [4], Shuang et al. [5], Stephen et al. [6], Anna et al. [7], Sila et al. [8], Yuehui et al. [9], Victor et al. [10], Hongkang et al. [11] and Jiwoong et al. [12]. This review article focuses on the self-assembly of nanostructured materials and the various interactions leading to self-assembly, with examples illustrating the role of these interactions. We then build upon the effect of the assembly on various properties. This review article gives a brief glimpse of these aspects to help a young researcher understand the concept of assembly and its effect.

Various Interactions Leading to Self-Assembly

In this process, weak interactions like H-bonding, electrostatic interactions, van der Waals and hydrophobic interactions play an important role in the formation of self-assembled structures. These forces are responsible for providing flexibility to the structures.

Hitasha Shahi and Jasveer Kaur have equal contribution.

✉ Sonalika Vaidya
svaidya@inst.ac.in

[1] Institute of Nano Science & Technology, Habitat Centre, Phase- X, Sector – 64, Mohali 160062, Punjab, India

Hydrogen Bonding

It is a special type of dipole–dipole attraction between molecules that occurs when a hydrogen atom is sandwiched between highly electronegative elements such as oxygen, nitrogen and fluorine. The hydrogen atom is covalently bonded with one of the electronegative elements. Due to this, the electron cloud of the electronegative element strongly attracts the electron cloud of the hydrogen atom, which makes the hydrogen positively polarized and interacts with the other electronegative atom. A schematic figure is shown in Fig. 1, to explain the interactions. This interaction is weaker than the covalent bond and stronger than the van der Waals forces. This bond is directional, which provides directionality and stability to the self-assembled structures.

We cite here a few examples that showcase the effect of H-bonding on the formation of assemblies. Meiling et al. [13] reported the assembly of Melem (2,5,8-triamino-heptazine) molecule on Ag(111) and Au (111) surfaces via hydrogen bonding. It was shown, with the help of STM (scanning tunneling microscopy), that when Melem was deposited on Ag(111), only one kind of structure was formed, whereas in the case of Au(111) two different appearances of the Melem molecule were obtained. Yu et al. [14] synthesized co-assembly of oligo (ethylene glycol) and gold nanoparticles, which were coated with an anionic polymer poly (acrylic acid). This assembly resulted in a change in the plasmonic properties of gold nanoparticles depending on the ratio of PAA/Au nanoparticles. No shift in the plasmon band was observed when the ratio was 1, indicating that there was no formation of co-assembly, whereas at intermediate ratios the peak was shifted to a longer wavelength suggesting the formation of co-assembled structures.

Electrostatic Interactions

It is a long-range order interaction that comes into existence when charged particles come closer to each other. Figure 2 shows a schematic that illustrates the nature of interaction associated when two charged particles are brought closer to each other.

Tianfu et al. [15] studied the assembly of positively charged Au and Fe_2O_3 nanoparticles on negatively charged multi-walled carbon nanotubes using electrostatic forces of attraction. These assemblies exhibited excellent performance toward generating energy for practical applications. Liuyang et al. [16] studied the equilibrium and dynamic behavior of a layer-by-layer assembly of charged Fe_2O_3 nanorods onto a charged superparamagnetic microsphere of COMPEL^{TM}, based on electrostatic forces of interaction. The authors claimed that the assembled structures could be used for various useful applications such as drug delivery, sensors, and vehicles. Yunxiao et al. [17] synthesized assembled fluorescent hybrid structure of gold nanoclusters and carbon dots via electrostatic interaction, which displayed dual emission behavior at the excitation wavelength of 380 nm. The authors claimed that these assembled structures could be used for intracellular imaging.

Van der Waals Interactions

These forces are originated by dipole or induced dipole interactions and are further classified into three different types [18]: (a) Keesam type occurring between two permanent dipoles (e.g., between methanol and chloroform), (b) Debye type occurring between a permanent dipole and an induced dipole (e.g., between acetone and hexane) and (c) London interactions occurring between two induced dipoles (e.g., between hexane and octane molecules). These interactions define the geometry and composition of the materials involved.

Yi et al. [19] synthesized the assembly of TiO_2 nanorods and SnO_2 nanowires on Ti_3C_2 sheets via van der Waals forces of interaction. The assembly leads to a decrease in the resistance to charge transfer, thereby increasing the transport of electrons and ions at the interface and hence could be used in lithium-ion batteries. Chenyang et al. [20] designed heterostructures by alternately stacking N-doped graphene and layered MoS_2 through van der Waals interactions. This assembly was shown to possess resistance toward charge transfer and acted as an anode material to be

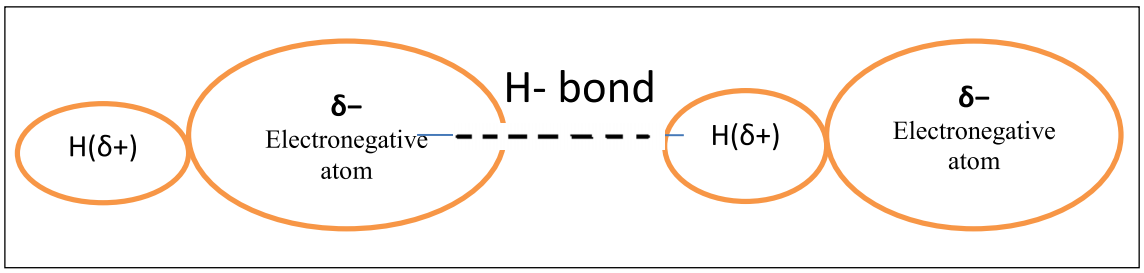

Fig. 1 Schematic showing the formation of a hydrogen bond

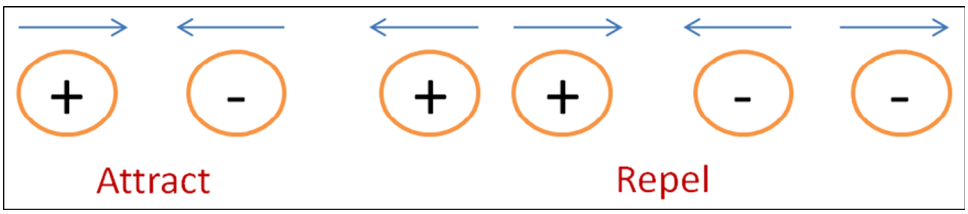

Fig. 2 Schematic showing the nature of the interaction between two charged particles

used in lithium-ion batteries. Mohadeseh et al. [21] synthesized the self-assembled structure of InAlAs and InAsP nanowires on graphene via pseudo-van der Waals interactions. The authors claimed that these structures can be exploited for various nanoelectronics and optoelectronic device applications. In 2013, Ying et al. [22] synthesized $Bi_2O_2CO_3$ with its structure close to the Aurivillius family, in which 2D nanosheets were formed by self-assembly arising as a result of the van der Waals interaction along the c-direction. These self-assembled structures were shown to have practical application in humidity sensing. These nanosheets of $Bi_2O_2CO_3$ were used in the humidity sensing tests, which shows high sensitivities in the impedance and capacitance by 3–4 orders of magnitude as compared to bulk Bi_2O_3, when the relative humidity was changed from 11 to 95%.

Hydrophobic Interactions

It is the type of interaction wherein there is a tendency of the nonpolar molecules to associate with each other in an aqueous media (Fig. 3). The hydrophobic effect is mainly entropic, but it is also affected by the enthalpy contribution, which is dependent on the change in the pressure and temperature.

Jong et al. [23] used these hydrophobic interactions to drive the self-assembly of gold nanoparticles with the block copolymer. The authors claimed that the assembly could be used as a nanoreactor, catalyst carrier, drug carrier, enzyme delivery agent, etc. Mukherjee et al. [24] demonstrated the assembly of gold nanoparticles on titanium dioxide thin films through hydrophobic and hydrophilic interactions, which resulted in better crystallinity and a decrease in the optical band gap in comparison with pristine TiO_2. The assembly could be used in light-harvesting and energy storage applications. Ana et al. [25] showed a new method for the self-assembly of gold nanoparticles into 3D clusters, which were driven by hydrophobic interactions. They have shown that by controlling the size and the distance between two particles, the optical response can be tuned. Thus, these kinds of assemblies may have the potential to be used for drug delivery purposes.

Other Factors

Apart from interactions, various environmental factors also affect the formation of assemblies. We list here two important factors, viz. the solvent and the temperature/pressure condition.

Effect of Solvent

Solvent plays a very important role in the assembly of nanostructures. The parameters of the solvent, which governs the assembly behavior, are viscosity, dielectric constant, coordinating ability of the solvent, polarity and steric hindrance. These parameters affect the solubility of the reactants, their reactivity and the crystallization kinetics. Eunhye et al. [26] reported the assembly of iron oxide nanoparticles on the supramolecular film of polystyrene-*block*-poly (2-vinylpyridine). They showcased the effect of solvent, viz. toluene, water and ethanol, and their mixture on the orientation of nanostructures. They also showed that the presence of a small amount of water changes the structural evolution of the thin film from a disorder-vertical cylinder to vertical lamellae, their mixture and finally cylindrical morphology. Anirban et al. [27] demonstrated the effect of solvent polarity (by using various solvents, viz. hexane, p-xylene, benzene, m-xylene, toluene, o-xylene and chloroform) on the rate of formation of cesium lead chloride and cesium lead bromide nanocrystals. It was shown that when the reaction for the formation of cesium lead bromide was carried out in chloroform, the

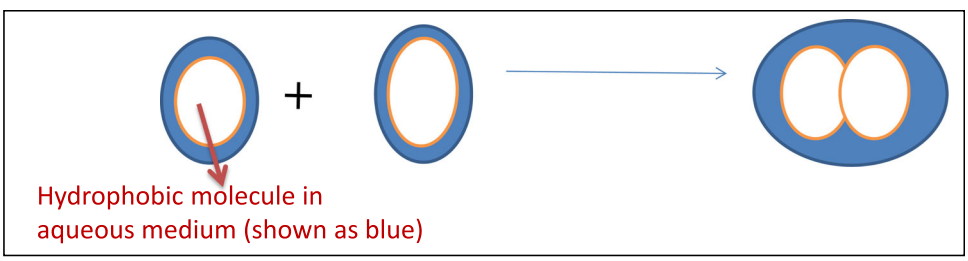

Fig. 3 Schematic showcasing hydrophobic effect in an aqueous medium

orthorhombic phase was formed. When the solvent was changed to hexane, pure trigonal phase of cesium lead bromide was formed. For cesium lead chloride, the crystal structure of the chloride formed was cubic, when the reaction was carried out in any kind of the solvents (hexane, p-xylene, benzene, m-xylene, toluene, o-xylene and chloroform). Apart from the structure, change in the solvent led to changes in the morphology of the particles. In chloroform, cubic-shaped nanocrystals were obtained, whereas in hexane, platelets were obtained. Wei et al. [28] studied the self-assembly behavior of Ph/NH_2-capped tetra (aniline) in 5 different organic solvents (THF, acetone, ethanol, DMF and DMSO). The authors observed the formation of spherical structures in THF, flower-like structures in acetone, nanocapsules in ethanol and nanowires in DMF and DMSO. They proposed that the assembly was formed due to hydrogen bonding as a result of solute–solvent interactions, which depend on the solvent polarity. The solvent also plays an important role in microemulsion-based synthesis. Microemulsions act as a template in governing the assembling behavior of the nanostructures [29]. This was demonstrated by Ganguli et al. [30] wherein they observed that with cyclohexane as the solvent, the aspect ratio of the nanorods of nickel oxalate was 6:1, whereas with hexane as the solvent, the aspect ratio decreased to 5:1. They attributed this change to the forces of interaction between the surfactant tail and solvent and interdroplet tail–tail interactions.

Effect of Temperature and Pressure

Jing et al. [31] studied the effect of temperature on the self-assembly of glycine on Cu (001). It was shown that the temperature affects the M-S interactions that govern molecular configuration. They reported that at 0 K these dominant interactions break and M-M interactions dominate, which determines the molecular arrangements. Yuxian et al. [32] studied the effect of both temperature and pressure on the self-assembled structure of silica particles to form opal films. They reported that the pressure required for obtaining optimal self-assembly depended on the size of the particles. The smaller-sized particles required higher negative pressure, whereas larger polydisperse particles required lower negative pressure. When the reaction was carried out at a temperature below the boiling point of the solvent, ordered closed-packed structures of SiO_2 were obtained, whereas in cases where the temperature was above the boiling point, particles were assembled irregularly. Yuan et al. [33] developed a sensitive pressure sensor from the self-assembly of polydimethylsiloxane film using polystyrene microspheres as a monolayer

Effect of Assembling on Physical Properties

The properties of assembled nanostructures arise as a result of the coupling effect. Here we discussed a few coupling effects with examples.

Coupling of Plasmons

Self-assembly of plasmonic nanoparticles results in highly tunable optical properties arising due to collective behavior. Such coupling of plasmon may find potential applications in the field of nanoscale lasing, plasmon-assisted photolithography, light-harvesting, photocatalysis and biological sensing. In metals (gold, silver, platinum, copper), a decrease in the size below the electron mean free path induces strong interaction between the light and the conduction electrons that are confined to a small volume of the metal particle. Under the influence of an oscillating electric field, the coherent oscillation of the free electrons from one surface of the particle to the other is called (localized) surface plasmons, which gives rise to intense absorption in the visible-near UV region. This is known as the surface plasmon resonance (SPR) absorption. When two plasmonic nanoparticles couple, there is splitting in the plasmon energies due to the intermolecular force of interactions, which results in the formation of bonding plasmon (results in a red shift in LSPR) and anti-bonding plasmon (results in a blue shift in LSPR frequencies). Klinkova et al. [7] reported that self-assembly of plasmonic nanoparticles is affected by the shape of individual nanoparticles, different methods of their assembly, type of capping ligands, solvent and intermolecular forces of interaction between the nanoparticles. Mattghias et al. [34] reported that by decreasing the interparticle distance between gold nanoparticles to a distance where they touch each other, nonlinear optical four-wave mixing is increased by 4 orders of magnitude. Song et al. [35] reported that Au nanoparticles could be self-assembled into nanoporous structures (nanoshells) by using redox-active polymer poly (vinylphenol)-b-(styrene) as a reducing agent. The authors demonstrated that as a result of the assembly formed, plasmonic “hot spots” at the surface were created, which enhanced the photothermal effect, surface-enhanced Raman scattering (SERS) and photoacoustic (PA) signals. The combination of these enhancements was used to obtain more accurate information about the tumors. Bian et al. [36] reported that due to highly ordered arrangement of Au nanoparticles, a strongly coupled electric field was produced, which resulted in strengthening the C-H peak due to the SERS effect, as observed from the anti-Stokes Raman spectra of dodecanethiol. A schematic is shown in Fig. 4 to explain the coupling of two plasmonic molecules. A new

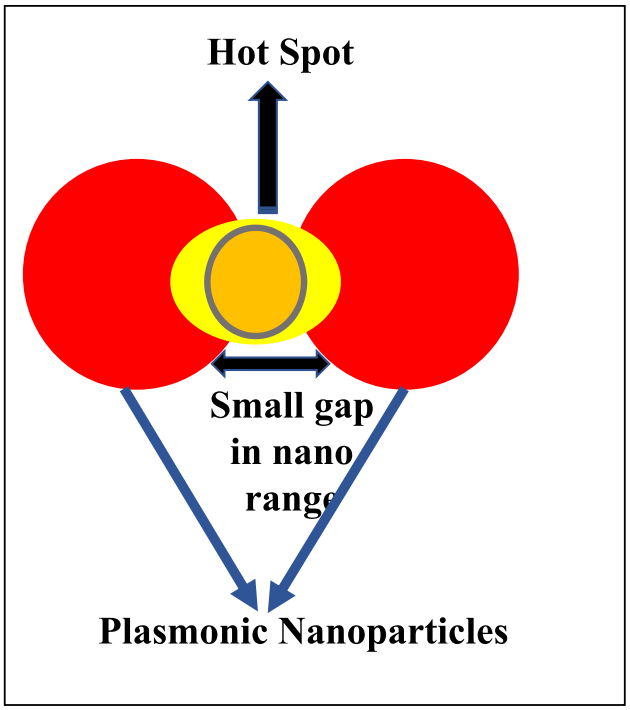

Fig. 4 Schematic showing creation of a hot spot due to plasmon–plasmon coupling

coupled excitation is formed when two plasmonic nanoparticles are coupled with each other. Hence, this coupling is spatially localized, resulting in the formation of 'hot spots', which has various sensing applications.

Coupling of Excitons

When two semiconductors are made to form an assembly, then their excitons couple with each other. Xienping et al. [37] reported that two semiconductors, viz. $MoSe_2$ and WSe_2, when coupled with each other, due to weak van der Waals forces of interaction, resulted in new photoluminescence (PL) peak. The authors justified the observation of a new peak to Coulomb attraction between the electrons in $MoSe_2$ and holes in WSe_2. Similarly to PL, the authors observed the renormalization of the vibrational motions in Raman spectra, which was not observed with individual $MoSe_2$ and WSe_2. Similarly, Moody et al. [38] also reported observation of a new peak in the PL spectra for self-assembled CdTe/CdMgTe, which was not observed with CdTe and CdMgTe only. Hence, this gives us an idea about how the self-assembly of two semiconductors affects their optical property. Recently, Darya et al. [39] reported that when TiO_2 nanotubes were assembled with Fe_3O_4 nanoparticles, then TiO_2 became photoactive in the visible region for degradation of methylene blue dye. A schematic is shown in Fig. 5 to explain the exciton–exciton coupling for various types of heterojunctions coupled to each other.

Coupling of Plasmon–Exciton

This type of coupling occurs when a metal nanostructure is conjugated with a semiconductor. This conjugation leads to a coupling of the plasmon, arising from metal nanostructure, with the exciton, created from the semiconductor. Bertoni et al. [40] reported that ZnO tetrapods were self-assembled with Au nanoparticles, which resulted in modification of the optical properties such as scattering, absorption and emission. It was shown that Au nanoparticles were used to enhance the optical properties of ZnO due to electromagnetic coupling between plasmon and exciton. The plasmonic nanoparticle resulted in the improvement of SERS sensitivity to adsorb various molecular systems on the metal nanoparticles due to which these metal–semiconductor systems could have potential applications in the field of biomedicine and optoelectronics. Abid et al. [41] reported that the radiative emission of $MoSe_2$ in the $MoSe_2$@Au hybrid system was enhanced by a factor of 10 as compared to bare $MoSe_2$ due to the presence of plasmonic Au nanoparticles in their vicinity. Neha et al. [42] synthesized SnO_2 nanostructures decorated with Au nanoparticles by the sputtering method. It was reported that excitons of SnO_2 coupled with surface plasmons of Au resulted in the enhancement of photoluminescence. Yang et al. [43] synthesized MoS_2/Ag hybrid system with enhanced optical properties, which were revealed by UV–visible transmission spectroscopy, fluorescence spectroscopy and SERS spectroscopy. It was reported that the holes of MoS_2 were occupied by plasmonic electrons having high kinetic energy, which makes the surface n-type due to which it has applications in the surface catalytic reactions. Figure 6 shows the schematic of plasmon–exciton coupling in which electromagnetic field gives rise to the collective oscillations, which results in surface plasmon resonances (SPRs), and it is then coupled to the excitons in the semiconductors.

Application of Assembled Nanostructures

Self-assembly of nanoparticles into 0D, 1D, 2D, 3D nanostructures has attracted many scientists due to their wide potential applications in the area of catalysis, magnetic, electronic and biomedical applications. Various metals, metal oxides and metal sulfides are self-assembled into hierarchical structures, resulting in the formation of nanostructures with controllable morphology. Randeep et al. [44] formed cauliflower-like nanostructures of AgCl and ZnO and showcased an enhancement of visible-light photocatalytic activity for the treatment of industrial wastewater. Liang et al. [45] reported the self-assembly of iron oxide into 3D flower-like porous nanostructures by

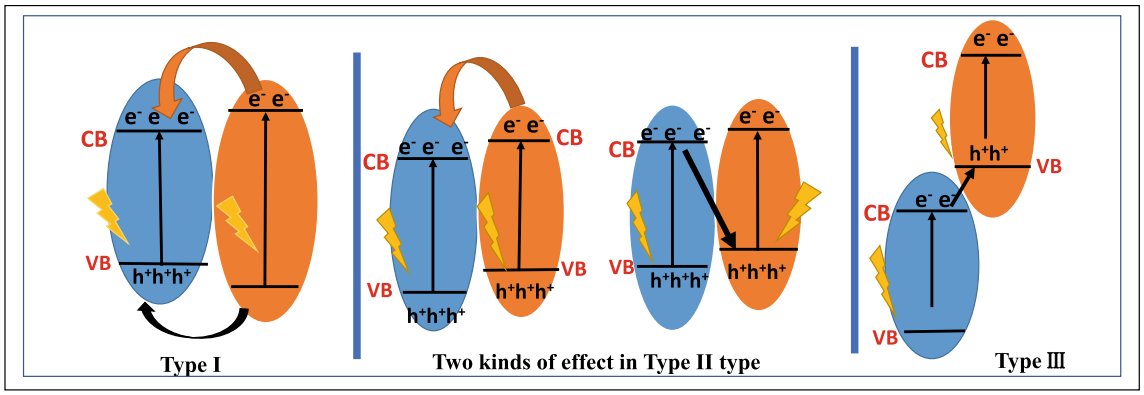

Fig. 5 Schematic showing the exciton–exciton coupling in various types of heterojunctions

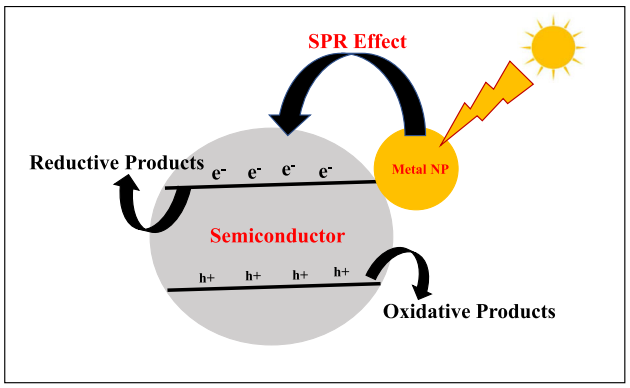

Fig. 6 Schematic showing the plasmon–exciton coupling

using ethylene glycol as a structure-directing agent. They used 3D flower-like nanostructures of iron oxide to remove toxic chemicals, pathogens and germs from the water. Lin et al. [46] proposed self-assembly of Bi_2O_3 into 2D nanosheets, which were inter-crossed with each other. They showed that the morphology, microstructure, pore size and self-assembly of Bi_2O_3 could be controlled by controlling the nucleation and growth behavior of nanostructures. It was also reported by the authors that self-assembled Bi_2O_3 nanosheets showed an enhancement in the photocatalytic activity up to 6–10 times when compared to that with commercial samples towards the degradation of RhB dye under visible light. Wang et al. [47] synthesized 3D flower-like Fe_3O_4@Bi_2O_3 core–shell structure by the solvothermal method. These 3D nanoflower-like structures were observed to be made up of nanosheets with a thickness of 4–10 nm and width 100–140 nm. These Fe_3O_4@Bi_2O_3 core–shell structures showed high photocatalytic activity for the degradation of RhB under visible light, which was 7–10 times higher than commercial Bi_2O_3. Xin et al. [48] synthesized self-assembled 3D microspheres of BiOI, which were formed from the assembly of nanoplatelets. These microspheres were shown to exhibit high porosity, narrow bandgap, high surface-to-volume ratio. These self-assembled BiOI showed higher photocatalytic activity toward the degradation of phenol in the visible light from its aqueous solution than random BiOI platelets. In 2018, Zaidi et al. [49] reported that spherical particles of ZnO, formed with the help of PEG-400, self-assembled with each other to form hollow spheres. It was proposed that the PEG-400 forms complex with Zn^{2+} ions in the solution. On heating, hydrolysis of Zn^{2+} ions occurred followed by the formation of assemblies to form hollow structures by the removal of PEG-400 during calcination. The self-assembled hollow nanostructures were shown to photodegrade the dye. Shaojun et al. [50] reported that FePt nanoparticles, having a particle size of 7 nm, when assembled on graphene by solution-phase self-assembly method, were found to be more active as a catalyst for the oxygen reduction reaction. Neing et al. [51] reported that self-assembly improves the surface area of the catalyst. It was shown that the assembly of Cu–TiO_2–SiO_2 increased the surface area when compared to that with bare TiO_2 and SiO_2. It was reported that this assembly resulted in an improvement in the reduction of CO to CO_2. Yang et al. [52] reported that the photocatalytic properties of $BiOCl_xBr_{1-x}$ were improved by self-assembly of nano-building blocks into ordered nanostructures, as a result of the increase in the surface-to-volume ratio, higher porosity and presence of various open active sites. It was reported that the 3D flower-like self-assembled nanostructures of $BiOCl_xBr_{1-x}$ have a high surface area due to which it showed enhanced photocatalytic activity towards the degradation of methyl orange in visible light. Jongam et al. [53] synthesized oleylamine-capped Ni and NiO, wherein the nano-building blocks self-assembled to form their ordered arrays. These self-assembled ordered arrays were used as a catalyst in the Suzuki coupling reaction.

Lithium-ion batteries have importance in electrochemical energy conversion and storage devices. Donghai et al. [54] formed assembled nanostructures consisting of nanocrystalline TiO_2 and graphene. These self-assembled nanostructures showed improved Li-ion insertion and extraction kinetics of TiO_2. The performance of the oxide

electrodes for electrochemical energy storage and conversion was also found to show an improvement. Yongming et al. [55] reported the self-assembly of MoS_2 – graphene nanoarchitecture without using any templates and organic additives. They showed that MoS_2 encapsulated into graphene sheets showed an enhancement in the cycling performance, rate capability, high coulombic efficiency and highly reversible capacity for lithium-ion batteries. Cao et al. [56] self-assembled V_2O_5 into hollow microspheres, which were shown to have improved electrochemical properties with higher efficiency and kinetic performance when used as the cathode in lithium-ion batteries. Shenglin et al. [57] synthesized self-assembled hexagonal nanosheets of Co_3O_4 having high surface area. It was reported that self-assembled Co_3O_4 nanosheets have wide potential applications in energy devices such as supercapacitors and lithium-ion batteries. Yonming et al. [58] synthesized self-assembled nanodisks of CoO having large surface area and open active sites, making them a potential candidate as long-life anode material for lithium-ion batteries with high reversible lithium storage capacity.

In another example [59], it was reported that by using a template-assisted self-assembly method, ultrathin nanosheets of NiO self-assembled with each other to form parallelly aligned NiO nanostructures. These self-assembled nanostructures exhibited a high active surface area for surface oxidation and reduction process. They also exhibited high current density and high stability and thus could be used as supercapacitors. Jiang et al. [60] reported the formation of self-assembly of stacked nanoplatelets and hexagonal nanosheets of $Ni(OH)_2$ nanostructures without the use of any template. These self-assembled nanostructures were shown to exhibit maximum specific capacitance of 1715 F g^{-1} with minimum potential of 0.6 V, thus finding a potential to be used as high-performance supercapacitors. Meng et al. [61] reported that self-assembled nanostructures could be used as fuel cells and energy storage devices. For illustrating this, they synthesized self-assembled nanostructures of copper- and cobalt-containing polypyrrole hydrogel. It was reported that these self-assembled hydrogels showed high electrocatalytic activity for the oxygen reduction reaction.

Thus overall, we have tried to give a brief glimpse of the area of self-assembly, which is an effective way for synthesizing nanostructures with new physical properties and functionalities. We believe that the knowledge of self-assembly, the interactions governing the assembly and their effect on the physical properties will allow researchers to synthesize nanostructures more robustly with precise control over their physical and structural properties.

Conclusion

In this review article, we have focused on various aspects that lead to the formation of self-assembly of nanostructures. The review summarizes various interactions leading to the self-assembly of nanostructures. We have cited various examples illustrating the effect of assembly on the physical properties, which arises as a result of the coupling effect. We have also cited few examples highlighting the potential use of assembled structures for various applications. We believe that the review will give a brief glimpse to young researchers and students about the area of self-assembly.

Acknowledgments HS and JK thank INST for fellowship. SV thanks CSIR (01(2943)/18-EMR-II), Govt. of India for financial assistance.

This paper is a revised and expanded version of an article entitled, 'Self-assembly nanostructured materials: Design and Mechanism of formation' presented in '7th International Conference on Advancements and Futuristic Trends in Mechanical and Materials Engineering' held at Indian Institute of Technology Ropar, Roopnagar, India, during December 5-7, 2019.

Authors Contribution HS contributed to the introduction and interactions part of the review. JK contributed to the physical properties and application of the review. The basic idea and the execution of the review article including corrections were carried out under the guidance of SV.

Compliance with Ethical Standards

Conflict of interest There is no conflict of interest to declare.

References

1. A.-C. Genix, J. Oberdisse, Soft Matter **14**, 5161 (2018)
2. A.P.U.D.K.B.G.P.S.R.G.S.P.S. Sivakumar, Self-Directed Assembly of Nanoparticles: A Review on Various Approaches. Advanced Theranostic Materials. **62**, 297 (2015)
3. H.S. Khoo, C. Lin, S.-H. Huang, F.-G. Tseng, Micromachines. **12**, 2 (2011)
4. Z. Nie, A. Petukhova, E. Kumacheva, Nat. Nanotechnol. **5**, 15 (2010)
5. S.-Y. Zhang, M.D. Regulacio, M.-Y. Han, Chem. Soc. Rev. **43**, 2301 (2014)
6. S. Mann, Nat. Mater. **8**, 781 (2009)
7. A. Klinkova, R.M. Choueiri, E. Kumacheva, Chem. Soc. Rev. **43**, 3976 (2014)
8. S. Toksoz, H. Acar, M.O. Guler, Soft Matter **6**, 5839 (2010)
9. Y. Wang, W. Zhou, J Nanosci Nanotech **10**, 1563 (2010)
10. V. Krivenkov, S. Goncharov, I. Nabiev, Y.P. Rakovich, Laser Photonics Rev. **13**, 1800176 (2019)
11. H. Wang, A.L. Rogach, Chem. Mater. **26**, 123 (2014)
12. J. Yang, K. Kim, Y. Lee, K. Kim, W.C. Lee, J. Park, FlatChem **5**, 50 (2017)
13. M. Bao, X. Wei, L. Cai, Q. Sun, Z. Liu, W. Xu, Phys. Chem. Chem. Phys. **19**, 18704 (2017)
14. Y. Torii, N. Sugimura, H. Mitomo, K. Niikura, K. Ijiro, Langmuir **33**, 5537 (2017)
15. T. Zhang, Z. Ma, G. Li, Z. Wang, B. Zhao, Y. Luo, J. Solid State Chem. **237**, 394 (2016)

16. L. Zhang, L. Zhu, S.R. Larson, Y. Zhao, X. Wang, Soft Matter **14**, 4541 (2018)
17. Y. Jia, X. Zhang, C. Yin, X. Zhang, J. Zhang, X. Wang, J. Xin, Anal. Methods **11**, 3974 (2019)
18. F.L. Leite, C.C. Bueno, A.L. Da Róz, E.C. Ziemath, O.N. Oliveira, Int. J. Mol. Sci. **13**, 12773 (2012)
19. Y.-T. Liu, P. Zhang, N. Sun, B. Anasori, Q.-Z. Zhu, H. Liu, Y. Gogotsi, B. Xu, Adv. Mater. **30**, 1707334 (2018)
20. C. Zhao, X. Wang, J. Kong, J.M. Ang, P.S. Lee, Z. Liu, X. Lu, ACS Appl. Mater. Interfaces. **8**, 2372 (2016)
21. M.A. Baboli, M.A. Slocum, H. Kum, T.S. Wilhelm, S.J. Polly, S.M. Hubbard, P.K. Mohseni, CrystEngComm **21**, 602 (2019)
22. Y. Zhou, H. Wang, M. Sheng, Q. Zhang, Z. Zhao, Y. Lin, H. Liu, G. Patzke, Sensors and Actuators B: Chemical **188**, 1312 (2013)
23. J.D. Jang, S.-W. Jeon, Y.-J. Yoon, J. Bang, Y.S. Han, T.-H. Kim, Polymer Chemistry **10**, 6269 (2019)
24. S. Mukherjee, M. Choudhuri, A. Datta, K. Koshmak, S. Nannarone, A.K. Mukhopadhyay (2017) Gold nanoparticle patterning on titanium dioxide thin films by hydrophilic and hydrophobic interactions effect on band gap, 2017 1st International Conference on Electronics, Materials Engineering and Nano-Technology (IEMENTech). 1.
25. A. Sánchez-Iglesias, M. Grzelczak, T. Altantzis, B. Goris, J. Pérez-Juste, S. Bals, G. Van Tendeloo, S.H. Donaldson, B.F. Chmelka, J.N. Israelachvili, L.M. Liz-Marzán, ACS Nano **6**, 11059 (2012)
26. E. Kim, S. Park, Y.-S. Han, T.-H. Kim, Polymer **150**, 214 (2018)
27. A. Dutta, R.K. Behera, N. Pradhan, ACS Energy Letters **4**, 926 (2019)
28. W. Lyu, M. Yu, J. Feng, W. Yan, ChemistrySelect **3**, 3338 (2018)
29. A.K. Ganguli, T. Ahmad, S. Vaidya, J. Ahmed, Pure Appl. Chem. **80**, 2451 (2008)
30. S. Vaidya, P. Rastogi, S. Agarwal, S.K. Gupta, T. Ahmad, A.M. Antonelli, K.V. Ramanujachary, S.E. Lofland, A.K. Ganguli, J. Phys. Chem. C **112**, 12610 (2008)
31. J. Xu, Z. Lin, S. Meng, J.-T. Wang, L. Xu, E. Wang, RSC Advances **7**, 4116 (2017)
32. Y. Zhang, M. Quan, W. Zhao, Z. Yang, D. Wang, H. Cao, W. He, Colloids Surf., A **529**, 832 (2017)
33. Y. Zhang, Y. Hu, P. Zhu, F. Han, Y. Zhu, R. Sun, C.-P. Wong, ACS Appl. Mater. Interfaces. **9**, 35968 (2017)
34. M. Danckwerts, L. Novotny, Phys. Rev. Lett. **98**, 026104 (2007)
35. J. Song, X. Yang, Z. Yang, L. Lin, Y. Liu, Z. Zhou, Z. Shen, G. Yu, Y. Dai, O. Jacobson, J. Munasinghe, B. Yung, G.-J. Teng, X. Chen, ACS Nano **11**, 6102 (2017)
36. K. Bian, H. Schunk, D. Ye, A. Hwang, T.S. Luk, R. Li, Z. Wang, H. Fan,(2018)
37. X. Fu, F. Li, J.-F. Lin, Y.-B. Gong, X. Huang, Y. Huang, H. Gao, Q. Zhou, T. Cui, J Phys Chem C. **51**, 122 (2018)
38. G. Moody, I.A. Akimov, H. Li, R. Singh, D.R. Yakovlev, G. Karczewski, M. Wiater, T. Wojtowicz, M. Bayer, S.T. Cundiff, Phys. Rev. Lett. **112**, 097401 (2014)
39. D. Beketova, M. Motola, H. Sopha, J. Michalicka, V. Cicmancova, F. Dvorak, L. Hromadko, B. Frumarova, M. Stoica, J.M. Macak, ACS Applied Nano Materials **3**, 1553 (2020)
40. G. Bertoni, F. Fabbri, M. Villani, L. Lazzarini, S. Turner, G. Van Tendeloo, D. Calestani, S. Gradečak, A. Zappettini, G. Salviati, Scientific Reports **6**, 19168 (2016)
41. I. Abid, A. Bohloul, S. Najmaei, C. Avendano, H.L. Liu, R. Péchou, A. Mlayah, J. Lou, Nanoscale **8**, 8151 (2016)
42. N. Bhardwaj, B. Satpati, S. Mohapatra, Appl. Surf. Sci. **504**, 144381 (2020)
43. X. Yang, H. Yu, X. Guo, Q. Ding, T. Pullerits, R. Wang, G. Zhang, W. Liang, M. Sun, Materials Today Energy **5**, 72 (2017)
44. R. Lamba, A. Umar, S.K. Mehta, W.A. Anderson, S.K. Kansal, J. Mol. Catal. A: Chem. **408**, 189 (2015)
45. L.S. Zhong, J.S. Hu, H.P. Liang, A.M. Cao, W.G. Song, L.J. Wan, Adv. Mater. **18**, 2426 (2006)
46. L. Zhou, W. Wang, H. Xu, S. Sun, M. Shang, Chemistry A. European Journal. **15**, 1776 (2009)
47. Y. Wang, S. Li, X. Xing, F. Huang, Y. Shen, A. Xie, X. Wang, J. Zhang, Chemistry A. European Journal. **17**, 4802 (2011)
48. X. Xiao, W.-D. Zhang, J. Mater. Chem. **20**, 5866 (2010)
49. Z. Zaidi, K. Vaghasiya, A. Vijay, M. Sharma, R.K. Verma, S. Vaidya, J. Mater. Sci. **53**, 14964 (2018)
50. S. Guo, S. Sun, J. Am. Chem. Soc. **134**, 2492 (2012)
51. W.-N. Wang, J. Park, P. Biswas, Catal. Sci. Technol. **1**, 593 (2011)
52. J. Yang, Y. Liang, K. Li, Y. Zhu, S. Liu, R. Xu, W. Zhou, J. Alloys Compd. **725**, 1144 (2017)
53. J. Park, E. Kang, S.U. Son, H.M. Park, M.K. Lee, J. Kim, K.W. Kim, H.-J. Noh, J.-H. Park, C.J. Bae, J.-G. Park, T. Hyeon, Adv. Mater. **17**, 429 (2005)
54. D. Wang, D. Choi, J. Li, Z. Yang, Z. Nie, R. Kou, D. Hu, C. Wang, L.V. Saraf, J. Zhang, I.A. Aksay, J. Liu, ACS Nano **3**, 907 (2009)
55. Y. Sun, X. Hu, W. Luo, Y. Huang, ACS Nano **5**, 7100 (2011)
56. A.-M. Cao, J.-S. Hu, H.-P. Liang, L.-J. Wan, Angew. Chem. Int. Ed. **44**, 4391 (2005)
57. S. Xiong, C. Yuan, X. Zhang, B. Xi, Y. Qian, Chemistry A. European Journal. **15**, 5320 (2009)
58. Y. Sun, X. Hu, W. Luo, Y. Huang, J. Mater. Chem. **22**, 13826 (2012)
59. J. Min, J. Liu, M. Lei, W. Wang, Y. Lu, L. Yang, Q. Yang, G. Liu, N. Su, ACS Appl. Mater. Interfaces. **8**, 780 (2016)
60. H. Jiang, T. Zhao, C. Li, J. Ma, J. Mater. Chem. **21**, 3818 (2011)
61. Y. Meng, J. Yin, T. Jiao, J. Bai, L. Zhang, J. Su, S. Liu, Z. Bai, M. Cao, Q. Peng, J. Mol. Liq. **298**, 112010 (2020)